

Sathickbasha K

Department of Mechanical Engineering
B S Abdur Rahman Crescent Institute of
Science and Technology, Chennai
India

Selvakumar A S

Department of Automobile Engineering
B S Abdur Rahman Crescent Institute of
Science and Technology, Chennai
India

Sai Balaji M A

Department of Mechanical Engineering
B S Abdur Rahman Crescent Institute of
Science and Technology, Chennai
India

Surya Rajan B

Department of Mechanical Engineering
B S Abdur Rahman Crescent Institute of
Science and Technology, Chennai
India

Effect of Steel Family Fibers on Friction and Stiction Behavior of Brake Pads

The study analyzes the effects of family of steel fibers on the thermo-mechanical, tribological and corrosive properties of Phenolic resin-based friction material. Tribological studies were performed on chase testing machine following SAE J661 standards. The brake seizure (corrosive stiction) due to corrosion is studied based on ISO 6315 test standard. The series of fibers used in this study include mild steel fibers, annealed steel fibers, and stainless steel fibers. The percentage by weight of fiber in all the composites was kept as constant at 12 % (Low metal series). For the purpose of comparison, another composite with 24 wt. % of stainless steel fiber was used in this study (High metal content). Experiments showed that the friction coefficient in general decreases with increasing temperature up to 300 °C and then was stable. Mild steel fiber reinforced composites fared better in fade and wear performance followed by annealed steel fibers. The highest friction (with poor consistency) and wear are found in the higher content of stainless steel fiber-based composite. Wear mechanism was studied by using scanning electron microscope.

Keywords: Friction; Wear; Stainless steel fiber; Annealed steel fiber; Stiction.

1. INTRODUCTION

Brake pad is a vital part of the automotive brake system. A good brake pad has to fulfill several functional requirements which include maintaining consistent friction level irrespective of the operating conditions, moderately low wear, resistance to corrosion, low noise and should not emit any toxic substances during braking [1–3]. Among the above properties, maintaining a consistency level of Coefficient of Friction (CoF) is challenging, as the temperature, speed, pressure and contact geometry keep on varying during dynamic braking [4]. Most of the brake pads are open to the atmosphere, to dissipate heat generated while braking. It leads to performance deterioration due to the presence of rain-water, sand and other foreign particles in the view of oxidation/corrosion aspects. Hence, to satisfy the numerous requirements, brake pads have more than ten ingredients in their formulations. Friction formulation ingredients are classified as binders, fillers (functional and inert), frictional additives/modifiers and reinforcing fibers [5]. Fibers provide structural integrity to the friction composite, so its importance is high.

During the usage of asbestos fibers, the fibers and fillers ratio is 60:40. After the ban of asbestos, the ratio changed tremendously to reduce the cost and to meet the ever-increasing requirements. As, a single fiber cannot be a direct substitute for asbestos, a variety of fibers are simultaneously used with balancing properties. Fibers available in the commercial sectors include man-made synthetic metal fibers (copper, brass,

bronze & steel) mineral fibers (rockwool, glass), organic fibers (Aramid, cellulose, acrylic, carbon), ceramic fibers and natural fibers (hemp, Prosopisjuliflora, jute, sisal, palm kernel shell, rice saw husk, etc.,) [6–8]. Natural fibers normally have poor heat resistance and not compatible with the resin and hence is still in the research level and not yet commercialized. Among various fibers, copper fibers are widely preferred in friction material because of its excellent thermal conductivity, good solid lubricant nature at high temperatures, low noise level, tendency to form friction film which aids in maintaining CoF and reducing wear. But, the environmental issues of the copper have resulted in a reduction of its usage in the brake friction material. Developed countries are making legislation policies to reduce the usage of copper in the formulation [9,10].

Steel fibers are normally used in the semi-metallic, full metallic and some extent in low metallic brake pads. The advantages of steel fiber are low cost when compared with other metal fibers, good thermal conductivity, excellent strength, good wear resistance, maintain friction effectiveness at elevated temperatures and better adhesion energy. However, steel fibers usage declined in the recent years as they tend to generate more noise and dust while braking. But, a revival for steel fiber usage came due to the restriction on copper and its alloys in friction materials and considered as a part of the substitute [11]. Most of the research article compares the steel fibers with the above-mentioned metal and mineral fibers and optimizing the steel fiber percentage in the formulation [12]–[17]. But a comparison of fibers among the steel family is not documented. So, the present work is mainly aimed to see the effect of various fibers in the steel family namely mild steel fiber, annealed steel fibers (stress relieved) and stainless steel fibers on the thermomechanical and tribological properties of friction materials.

Received: December 2018, Accepted: March 2019

Correspondence to: Mr Sathickbasha K,
B S Abdur Rahman Crescent Institute of Science and
Technology, Chennai, India

E-mail: sathick.basha@crecsent.education

doi:10.5937/fmet1904856S

© Faculty of Mechanical Engineering, Belgrade. All rights reserved

FME Transactions (2019) 47, 856-864 856

In the present work, four brake pads are developed by keeping the parent formulation fixed and varying only the different steel fiber content and are named as MSFBP (Mild steel fiber based brake pad), ASFBP (Annealed steel fiber based), LSSBP (Lesser content (12%) of Stainless steel fiber based), HSSBP (Higher content (24%) of stainless steel fiber based). The thermal conductivity and diffusivity of the brake pads have very much influence on the tribological properties [18,19]. So, the thermal conductivity and diffusivity of the brake pads were studied based on ASTM E1461. Friction and wear studies are tested in chase friction /wear testing machine following SAE J661 standards. Wear mechanism is analyzed using SEM. Even though ferrous materials are very prone to environmental corrosion, its usage cannot be avoided in the friction material formulation.

The formulation uses various anti-corrosion compensators like sodium nitrite and alkanolamine-carboxylic acid salts to avoid the stiction seizure of pad with the rotor. Ferrous brake seizure due to corrosion test using the schedule ISO 6315 is also performed to evaluate the corrosion/stiction resistance. This test enables the corrosion nature of the various ferrous fibers in this study [20,21].

2. MATERIALS AND EXPERIMENTAL METHOD

2.1 Materials

The mild steel fiber was procured from Frimart, Ghaziabad, India. The annealed steel fiber and stainless steel fiber were procured from Chiao Yu Friction Co., Ltd. Taiwan. Figure.1 shows the microscopic view and surface morphology of the MS, AS and SS fibers. The chemical composition of fibers is shown in Table 1. The general specification of the steel family fibers is in Table 2.

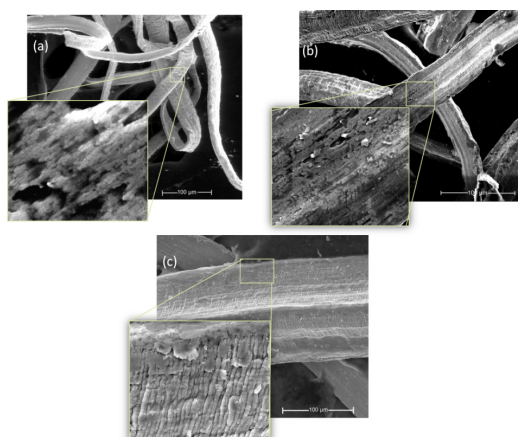


Figure 1. SEM Micrograph of metal fiber: (a) Mild Steel Fiber, (b) Annealed Steel Fiber, (c) Stainless Steel Fiber.

Table 1. Composition of the metallic fibers.

Chemical Elements	Composition (%)							
	C	Si	Mn	Cr	Mo	P	S	Ni
Mild Steel fiber	0.07-0.12	<0.6	<0.6	0	0	<0.05	<0.05	-
Annealed steel fiber	0.07-0.12	<0.2	<1.25	0	0	<0.05	<0.05	
Stainless Steel fiber	0.08	<1	<1	16-18	0.75-1.25	<0.035	<0.03	

Table 2. Material specifications from the supplier data sheet.

Properties	MSF	ASF	SSF
Specific Gravity (g/cc)	7.8	7.8	9.5
L/D ratio	10-15	10-15	10-15
Thermal Conductivity (Wm ⁻¹ k ⁻¹)	34-55	34-55	18-26
Hardness (Raw material) Rockwell 'B' scale	71	71	95

2.1.1 Brake Pad Fabrication and Characterization

The fabrication of brake pads carried out in Frimart Ghaziabad and contained 15 FM ingredients. The parent FM formulation contains fibers 23% (Aramide pulp, PAN- Poly Acrylonitrile, Glass, Copper-fiber), Abrasives 8% (Al₂O₃, Cashew Friction dust), Lubricant 20 % (Synthetic-Graphite, MoS₂, SnS₂) Filler 5 % (Ca(OH)₂, CaCO₃) and Binder 14% (Phenolic Resin, NBR). The brake pad compositions and its variations are shown in Table 3. The ingredients were mixed using the industrial plough shear mixture for 9 minutes. The mixed ingredients were poured into the single cavity brake die for Mercedes Benz S class vehicle. The curing took place at the temperature of 156 °C and the fluid pressure of 10 MPa. Then the pads were post cured at 150 °C for 4 Hrs [22].

Table 3. Brake pads compositions.

Ingredient Wt (%)	MSFBP	ASFBP	LSSBP	HSSBP
Low Metal Series				
Parent Ingredient	70	70	70	70
Baryte	18	18	18	6
MSF	12			
ASF		12		
SSF			12	24

The Hardness of the samples was measured using Rockwell hardness tester using L scale. The thermal conductivity and diffusivity of the brake pad samples were studied using LFA 467 Hyperflash tester.

2.2. Friction & Wear Test

The brake pad friction material sized to 25x25x8 mm sample and the test schedule is given in Table 4. The facing side of the sample slides against the cast-iron rotor in the chase friction tester. The test procedure starts with burnishing cycle, which ensures the sliding contact of the pad and the rotor. The friction performance (CoF) recorded for 20 cycles in the baseline-1. The important performance study fade-1 starts after baseline-1, which evaluates the friction performance over the temperature range of 82-289 °C. Heating coils surround the rotor increases the temperature. Once the temperature reaches 289 °C the heating coils stops heating, the blower starts reducing the temperature and this cycle named as Recovery-1.

Wear cycle followed by the recovery-1, evaluates the wear thickness loss of the brake pad sample over 100 brake applications with the dead load of 657 N. Similarly the Fade-2 and Recovery-2 cycle runs with continuous drag over the temperature range of 82-345

°C and 317-93 °C respectively. Finally, the baseline-2 cycle evaluates the CoF of the brake pad for 20 brake applications in the absence of thermal load. The surface roughness of tested specimens (worn surface) are measured using Surface Roughness Tester-Taylor Hobson -16 nm Resolution.

Table 4. SAE J661 test schedule.

S.No	Test Name	No of brake applied	Temperature Range(°C)
1	Burnishing (20 minutes)	1	-
2	Baseline-1	20	82-104
3	Fade-1	1	82-289
4	Recovery-1	1	261-83
5	Wear cycle	100	80-100
6	Fade-2	1	82-345
7	Recovery-2	1	317-93
8	Baseline-2	20	82-104

2.3 Stiction test

The corrosion of the brake disc and pad interface sticks the pad with the rotor. Due to this corrosion stiction (seizure condition) of the pad and rotor, the liner removal from the backplate takes place unexpectedly. This corrosion-condition is simulated based on the standard ISO 6315. The brake pads and rotor surface are cleaned to ensure it is free of dust. The MSFBP, LSSBP, HSSBP, were immersed in the solution contains 5% NaCl, 0.5% MgCl, and 0.5% CaCl₂ solution for 10 minutes. The pads are kept in the humidity chamber with 95±3 % of relative humidity at 50±2 °C for 4 hours. Then the rotor is kept in the same chamber for 30 minutes. The excess moisture is removed using a moisture absorbent paper in brake pad surfaces and the rotor contact surface. The pads are placed on the surface of the rotor and held by clamps (Figure 2 (a)). The assembled set is then placed in the humidity chamber of the same RH and temperature for 72 hours as shown in Figure 2 (a).



Figure 2. Brake pad and rotor assembly for stiction test placed in the humidity chamber.

Then, the setup is removed from the humidity chamber and kept in the room temperature of 37 °C with a relative humidity of 70 % for 48 hours. After 120 hours of corrosion test the rotor and the pad stick to each other. Steadily increasing force removes the test pads. The maximum force required to detach the pad from the rotor was recorded. The process is applied to all the pads to

calculate the breakaway force required [20]. The detached rotor and the brake pads are shown in Figure 2 (c) and (d).

3. RESULTS AND DISCUSSION

3.1 Characterization of Brake Pads.

The hardness and thermal properties of the BFCs are tabulated in Table 5. The hardness of the HSSBP are higher because high steel fiber content [23] than other low metal series brake pads which are showing negligible variation.

The thermal conductivity of the MSFBP and ASFBP is higher than the stainless steel brake pads LSSBP and HSSBP because the thermal conductivity of the stainless steel is lower than the MSF and ASF (Table 3 and Table 5). A similar variation is recorded for the thermal diffusivity also.

Table 5. Properties of BFCs.

Properties	MSFBP	ASFBP	LSSBP	HSSBP
Hardness (HRL)	80-96	88-96	80-88	90-98
Thermal Conductivity (W/m. K)	2.12	2.08	1.83	1.91
Thermal Diffusivity (cm ² /s)	0.0068	0.0063	0.0053	0.0053

3.1.2 Surface Roughness

The surface roughness of the brake pad's contacting face was tested after the friction test is shown in Table 6. The average roughness (R_a) of the brake pads is varying with the type of steel fiber. HSSBP has shown the highest roughness value because of the abrasive nature of a counterpart. In low metal series friction composites, MSFBP shows the lowest roughness and LSSBP shows the highest roughness. The roughness values R_t and R_z show the same pattern of variation concerning the type of steel fiber.

Table 6. Surface roughness R_a, R_t and R_z of Brake Pads.

Roughness	MSFBP	ASFBP	LSSBP	HSSBP
R _a	2.7678	2.8599	3.5420	6.5008
R _t	25.8418	30.2436	40.1038	75.2855
R _z	17.2895	18.8605	21.2255	36.3018

3.2. Effect of Rotor Temperature on CoF (Fade Cycle)

According to Blau [24], stable friction behavior characterizes a good brake pad. The fade cycle is characterized by the difference in the μ value, and the magnitude of the difference varies highly depending on the ingredients in the formulation [25]. The variation of μ is the function of sliding speed and the applied pressure [26] which directly influences the temperature rise at the interface of the brake pad and rotor [27], [28]. As seen from Figures 3 a and b, upto 120 °C all the developed friction composite samples gain the μ value. This is in accordance with the results of P.D.Neis et al. [29] who demonstrated the increase in the mean area of plateaus is responsible for the increase in μ from braking number 0 (untested pad material) to 50 respectively.

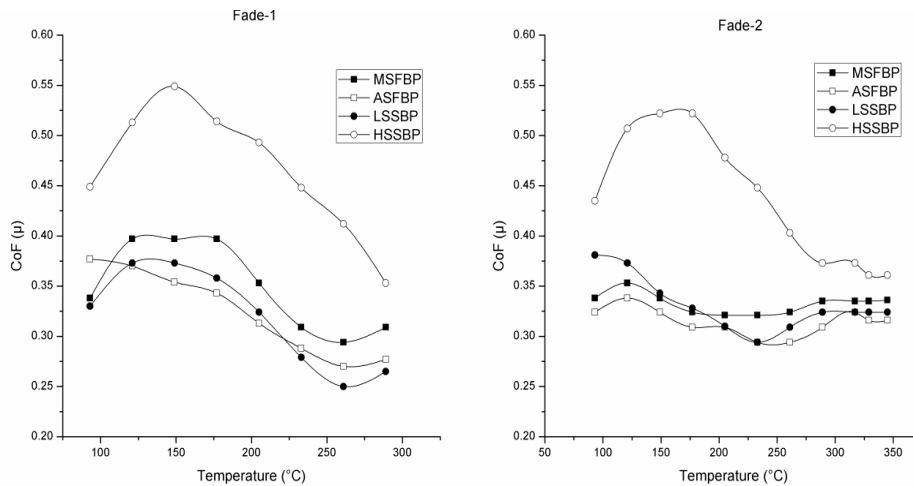


Figure 3. CoF variation with respect to Temperature (a) Fade-1 cycle (b) Fade -2 cycles.

In the case of HSSBP, μ increased upto 0.55 due to its high surface roughness value. Roughness dictates the contact area and contact stresses. Significant difference in R_a value observed between low metal series brake pads and high metal fiber brake pads (ref. Table 6). This indicates that the surface grooving kind of friction mechanism between the peaks of rotor and pad plays a significant role in increasing the μ value in HSSBP [30], or in other words for rough surfaces, the friction is high because of the need to lift one surface over the asperities [31]. When the rough surface of the brake pad was worn, the primary plateaus are formed, which tend to increase the possible real area of contact between the pad and the rotor [32].

This abrasive nature increases the flash temperature at the interface rapidly which cause early declining of μ in the HSSBP. Further, the formation rate of oxides due to the flash temperature at the interface lubricates the surface between the pad and the rotor which contributes to reducing the friction [11].

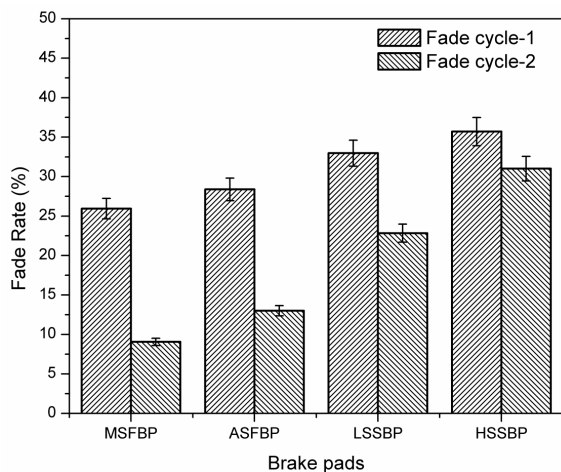


Figure 4. Percentage Fade Rate of the brake pad samples.

In the case of low metal fibers, there is no significant relationship observed between the roughness and friction level. After 150 °C, irrespective of the steel fiber type and wt. % in the FC formulation, μ reduces in the fade-1 and fade-2 cycle. The change/reduction in μ is expected due to the change in the plastic deformation and adhesion resistance of dry sliding friction materials with respect to temperature [33,34]. The HSSBP shows the first decline in μ compared to the other low fiber FCs; this is due to rapid increase in temperature (°C/sec) at the interface. The increase in metal content in the formulation increases the abrasive nature of the FC [12].

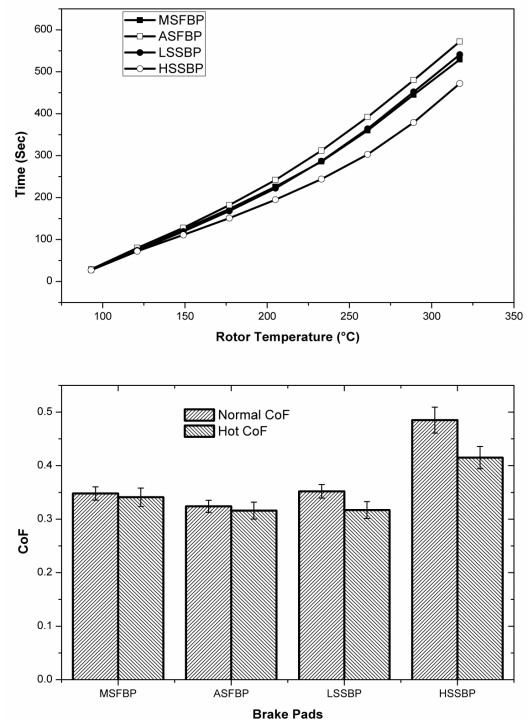


Figure 5. Rotor Friendliness analysis: (a) Time Vs. Rotor Temperature in Fade-2 cycle, (b) Normal and Hot CoF.

All the low metal fiber content brake pads also showed the decline in μ after 150 °C. Since all the brake pads were fabricated with steel fiber family, it can be attributed to the destruction of the transfer-film by the abrasive action of the steel fibers, which is accountable for the coefficient of friction stabilization [5,35]. Among the low metal composites, SSFBP shows the lowest μ (0.27). Since the thermal conductivity of the SSF is lower than MSF and ASF, the MSFBP shows higher μ in the fade cycles (ref. Figure 3). The low

thermal conductivity of the SSF weakens the interstitial bond between the polymer and fiber by accumulating heat on the friction surface [36]. The accumulated heat increases the interface temperature between the rotor and pad, which cause higher % fade rate in LSSBP as shown in Figure 4. Further, stainless steel fiber has more hardness than the other two versions. In spite of having hardness more than its counterparts, μ declined which is in agreement with the work carried out by wang et al., who compared mullite and steel fiber [37]. Even though the mullite is harder than steel fiber, the mullite fiber based brake pad produced lower frictional values the reason being attributed to poor plastic deformability, which reduces the ability of the metal to adhere, resulting in low friction.

The increase in metal fiber content also increases the overall thermal conductivity of the BP, since the fade cycle is continuously sliding. The increase in thermal conductivity of HSSBP doesn't provide friendliness with the rotor, which is contradictory to the observation done in the work of [36]. Also, the presence of high SSF in HSSBP increases the surface roughness value of the BFC (ref. Table 6) which subsequently increases the abrasive-wear as well as does high damage to the rotor [15].

3.3 Wear

Wear of brake pad regarding % thickness loss and % weight loss plotted in the graph shown in Figure 6. The wear loss calculated after all cycle of tests completed as per SAE J661 schedule. In low steel brake pad series, MSFBP has the lowest wear loss compared to others BPs. LSSBP has the highest wear thickness loss. From Table.6, it can be inferred that the increased brittleness of the stainless steel fiber increases the scratches on the rotor surface by which it increases the average surface roughness of the rotor-sliding track. The higher surface roughness and the low rotor friendliness (ref. Figure.5) of the LSSBP cause more rapid wear than other low metal friction composite, whereas in the case of ASF and MSF BPs the wear resistance is higher. Due to the ductility of MSF and ASF, the metal surfaces has the ability to plastically deform and move from the brake pad surface to rotor and back to the pad surface [38].

This mechanism eventually forms the oxide layer on the rotor and pad surface. In the case of SSF, the plastic deformation is not happening to cause the film transfer. The film transfer mechanism plays a major role in defining the wear performance of the brake friction composite. The huge difference is observed between low metal BP and high metal BP in wear loss percentage. Wear loss of HSSBP is almost more than twice as low metal BP. As inferred from the rotor friendliness and the friction character of the BPs, the temperature rise at the interface and the average friction level of HSSBP is higher than other BPs, which is responsible for the high wear rate in the case of high metal [27], [39].

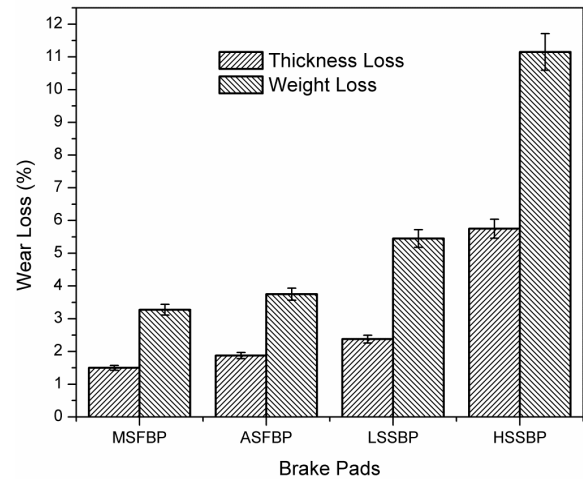


Figure 6. Wear loss analysis: Percentage Thickness loss and Percentage weight loss.

3.3.1 Worn Surface analysis

Worn surface analysis conducted on the brake pads to understand the mechanisms of wear during the dry sliding of brake pad against the cast-iron rotor. The SEM images of the worn surface shown in Figure 7 were taken at 300x magnification. In the entire BPs, the primary (directly contacted surface of the metal fiber, filler or Hard abrasive) and smooth secondary plateaus are visible and marked as A and B respectively.

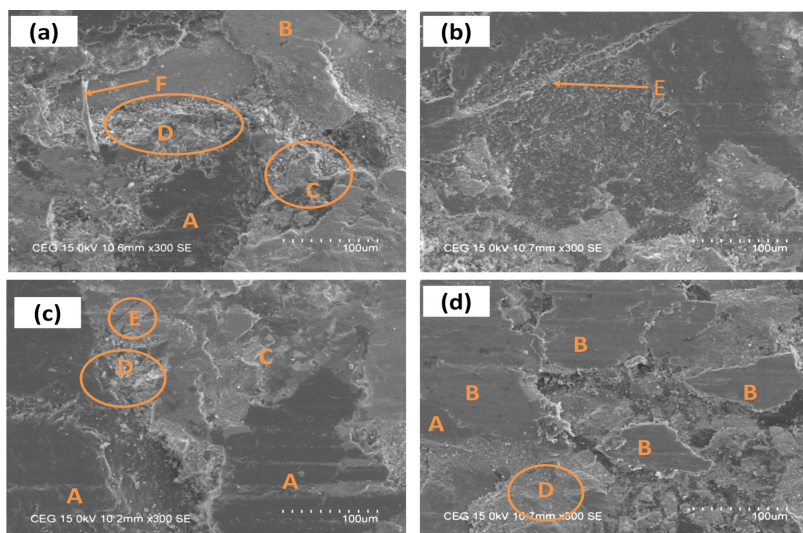


Figure 7. SEM micrograph of worn surface of BPs (a) MSFBP, (b) ASFBP, (c) LSSBP and (d) HSSBP.

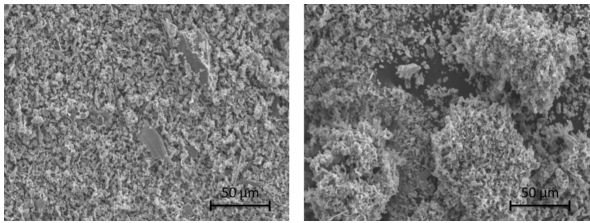


Figure 8. Wear debris collected from brake pad sample (a) LSSBP and (b) HSSBP.

Figure 7(a) shows that the surface of MSFBP filled with multiple secondary layers (due to the back-transfer of ultrafine wear fragments) adheres to the rotor and pad [11,32,40,41] which also supports low wear of the MSFBP. The fragmented third body particles (marked as D) grow into the secondary tribo layer (due to tribo back transfer) that is visible in the SEM image of MSFBP [42]. The MSFBP also shows the presence of compactly packed secondary plateaus which reduces the direct contact of pad bulk material with the rotor which makes the MSFBP samples rotor friendly (ref. Figure 5a). The size of the primary layer (A) is higher in the case of LSSBP, and the wear track grooves on the primary plateaus are clearly visible.

These indications clearly state the abrasive nature of the LSSBP compared to other low metal series brake pads. The abrasive nature of LSSBP is also justified with the roughness value (higher than other low metal series) taken perpendicular to the sliding direction (ref. Table 6). The micrograph of HSSBP (Figure 7d) indicates the loosely packed secondary plateaus which can be removed due to adhesive peel-off [43].

Also the layer peel-off increases the direct contact of metal fibers with the cast iron rotor, which is responsible for a high-temperature rise at the sliding interface and the less rotor friendly-ness compared to low metal samples. The detachment of secondary plateaus creates larger wear debris as shown in Figure 8 (few hundred microns), which do not help to back transfer fragments that are mainly responsible for high wear in HSSBP [43]. The fiber peel-off region marked as F which is due to the irregular orientation of fiber and due to abrasive plowing of the rotor against the pad.

3.4 Effect of Mild steel fiber and quantity of stainless steel fiber on corrosion study

The breakaway force for the different brake pads is tabulated in Table 7. The breakaway force for the MSFBP is higher as expected. The corrosive sticking is very high due to the corrosive nature of MS fiber compared to stainless steel fiber.

Table 7. Breakaway force required to detach the sticking pads with the rotor.

Brake pads	MSFBP	LSSBP	HSSBP
Breakaway force	156 N	77 N	121 N

The high stainless steel content also increases the breakaway force compared to low stainless steel brake pads. ASF has very similar chemical composition and crystal structure with MSF, so the annealed steel based brake pad is not considered for the corrosive study. As inferred from microscopic study (Figure 9), MSFBP has more corroded surface when compared to LSSBP and HSSBP.

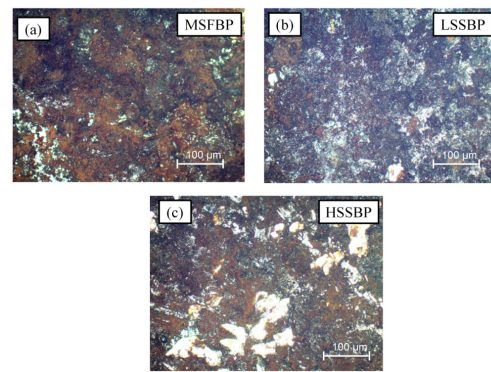


Figure 9. Optical microscope image of the brake surface after stiction test.

Contact surfaces in MSFBP have more corroded layers with more evidence of oxidized surface; it is due to the corrosive behavior of the rotor (cast iron) and the MS fibers in contact. In HSSBP the corrosive layers are less, and the fibers are evidence that the oxidation between the rotor and pad surface is minimum in HSSBP when compared to MSFBP. The low metal LSSBP has the lowest corrosion rate as observed in the figure 9. It is due to the non-corrosive nature of the stainless steel fiber.

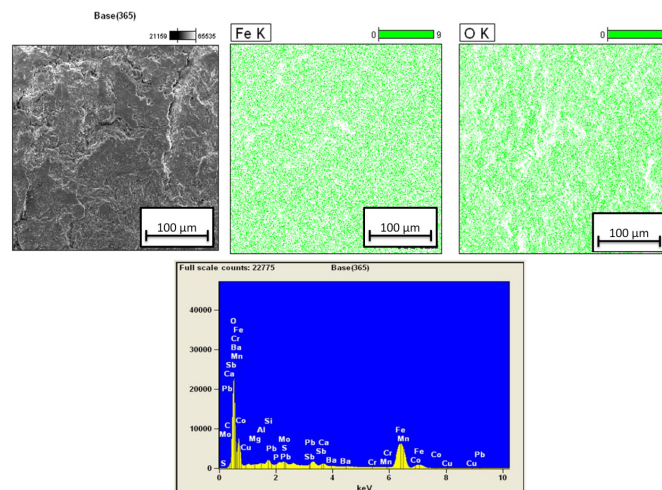


Figure 10. SEM Morphology and Energy dispersive X-ray spectrometry mapping on the corroded surface of the MSFBP with the rotor.

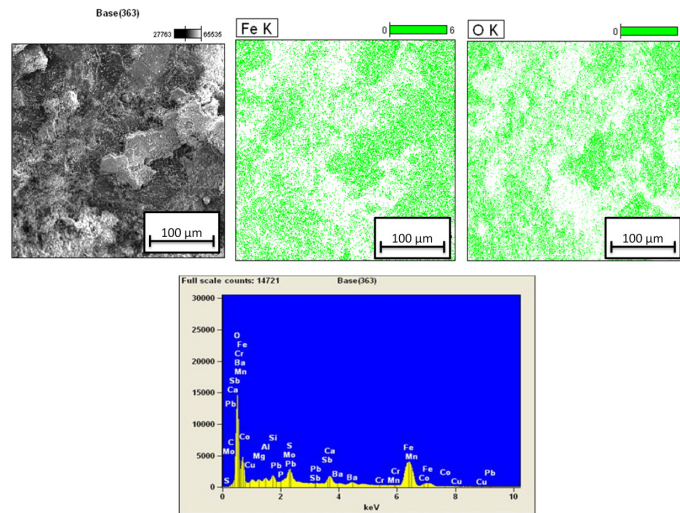


Figure 11. SEM Morphology and Energy dispersive X-ray spectrometry mapping on the corroded surface of the LSSBP with the rotor.

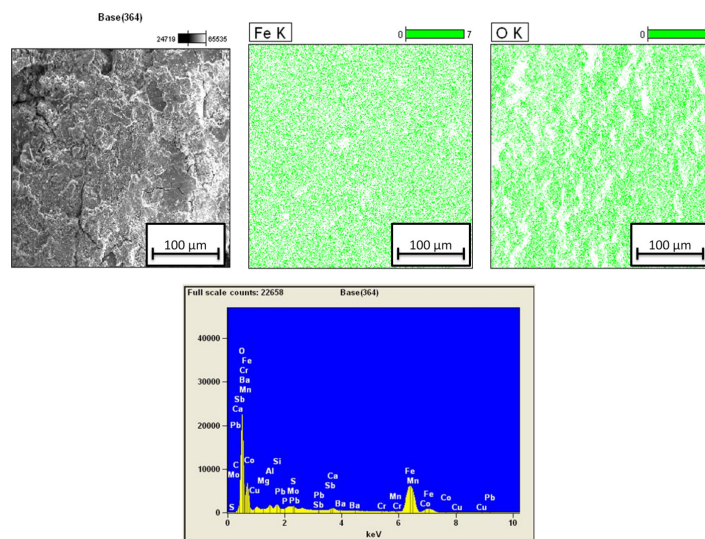


Figure 12. SEM Morphology and Energy dispersive X-ray spectrometry mapping on the corroded surface of the HSSBP with the rotor.

Figures 10-12 show the scanning electron microscopy micrograph and EDX elemental (Fe, O, etc.) distribution of the corroded surfaces after stiction test (ISO 6315). The elemental distribution of the MSFBP shows the highly dense distribution of Fe and O on its surface. These Fe and O dots represent the corroded layer transfer from the disc to BFCs. Also, the adsorption capacity of this composite is high which causes the corroded layer to transfer from the disc to the BFC. Hence, it infers that the corroded layer transfer from the disc to the BFC is very high in the case of MSFBP. Figure 11 shows that the LSSBP has a low corroded layer transfer when compared with MSFBP and HSSBP. The real surface area of the corroded layer over the FC surface is directly proportioned to the load required to detach the brake pad from the rotor (ref. Table 7). Even though the stainless steel fiber plays a vital role in minimizing the corrosion rate at the interface of the pad and rotor, the real area of the corroded layer is high in the case of HSSBP compared to LSSBP. It shows that the high metal content in the FC increases the corrosion layer transfer and adhesion breakaway force as observed in the ISO 6315 stiction test.

4. CONCLUSION

In this study, we investigated the effect of different fibers (mild steel, annealed steel, and stainless steel) in the brake pad on the mechanical, corrosion and friction characteristics by testing as per industrial standards.

The following notable outcomes were made from the study.

- The MSF and ASF based brake pads performed better in the high temperature braking cycles. Their fade resistance is better than the SSF based brake pads.
- Even though HSSBP achieved the highest friction, its poor stability makes it vulnerable to extreme conditions.
- Thermal conductivity and surface roughness of MSFBP play a convincing role in controlling the friction mechanism of the metal fibers.
- Corrosion resistance of the MSF reinforced brake pad is poor than SSFBP, hence SSF brake pads can be used for parking brakes to minimize seizure.
- Adhesion and abrasion mechanism controls the wear behavior. In particular, during abrasion, plowing and micro cutting was observed to be the

dominant mechanism in controlling the wear of the brake pads.

The detailed study by using the cocktail of these fibers is the future scope for this work.

REFERENCE

- [1] W. Österle *et al.*, “A comprehensive microscopic study of third body formation at the interface between a brake pad and brake disc during the final stage of a pin-on-disc test,” *Wear*, vol. 267, no. 5–8, pp. 781–788, Jun. 2009.
- [2] A. L. Cristol-Bulthé, Y. Desplanques, G. Degallaix, and Y. Berthier, “Mechanical and chemical investigation of the temperature influence on the tribological mechanisms occurring in OMC/cast iron friction contact,” *Wear*, vol. 264, no. 9–10, pp. 815–825, 2008.
- [3] R. Yun, P. Filip, Y. Lu, “Performance and evaluation of eco-friendly brake friction materials,” *Tribol. Int.*, vol. 43, no. 11, pp. 2010–2019, Nov. 2010.
- [4] S. J. Kim and H. Jang, “Friction and wear of friction materials containing two different phenolic resins reinforced with aramid pulp,” *Tribol. Int.*, vol. 33, no. 7, pp. 477–484, Jul. 2000.
- [5] D. Chan, G. W. Stachowiak, “Review of automotive brake friction materials,” *Proc. Inst. Mech. Eng. Part D J. Automob. Eng.*, vol. 218, no. 9, pp. 953–966, Sep. 2004.
- [6] M. A. S. Balaji and K. Kalaichelvan, “Optimization of Organic Fibres%[Kevlar/Arobocel/Acrylic] in NAO Brake Pad Application and its Effect on Thermal Stability & Friction Characteristics,” *Key Eng. Mater.*, vol. 531–532, pp. 8–12, 2012.
- [7] X. Li, W. Yue, Z. Fu, H. Huang, C. Wang, and J. Liu, “Tribological behaviors of W/Mo films under lubrication of zinc dithiophosphates – understanding their roles in tribochemical reactions,” *Tribol. Trans.*, vol. 0, no. 0, pp. 1–36, 2018.
- [8] B. Surya Rajan, M. A. S. Balaji, S. S. Saravananakumar, “Effect of chemical treatment and fiber loading on physico-mechanical properties of Prosopis juliflora fiber reinforced hybrid friction composite,” *Mater. Res. Express*, vol. 6, no. 3, p. 035302, Mar. 2019.
- [9] C. C. Engberg, “The Regulation and Manufacture of Brake Pads: The Feasibility of Reformulation to Reduce the Copper Load to the San Francisco Bay,” no. July, pp. 1–27, 1995.
- [10] C. Cantoni, R. Cesarini, G. Mastinu, G. Rocca, and R. Sicigliano, “Brake comfort - A review,” *Veh. Syst. Dyn.*, vol. 47, no. 8, pp. 901–947, 2009.
- [11] R. C. Dante, *Handbook of friction materials*. 2016.
- [12] S. Bin Park, K. H. Cho, S. Jung, and H. Jang, “Tribological Properties of Brake Friction Materials with Steel Fibers,” vol. 15, no. 1, pp. 27–32, 2009.
- [13] M. Kumar and J. Bijwe, “Role of different metallic fillers in non-asbestos organic (NAO) friction composites for controlling sensitivity of coefficient of friction to load and speed,” *Tribol. Int.*, vol. 43, no. 5–6, pp. 965–974, 2010.
- [14] Y. Lu, C. F. Tang, Y. Zhao, and M. A. Wright, “Optimization of a semimetallic friction material formulation,” *J. Reinf. Plast. Compos.*, vol. 23, no. 14, pp. 1537–1545, 2004.
- [15] M. Kumar and J. Bijwe, “Optimized selection of metallic fillers for best combination of performance properties of friction materials: A comprehensive study,” *Wear*, vol. 303, no. 1–2, pp. 569–583, 2013.
- [16] S. Bagheri Kazem Abadi, A. Khavandi, and Y. Kharazi, “Effects of mixing the steel and carbon fibers on the friction and wear properties of a PMC friction material,” *Appl. Compos. Mater.*, vol. 17, no. 2, pp. 151–158, 2010.
- [17] K. Sathickbasha, A. S. Selvakumar, M. A. S. Balaji, and B. S. Rajan, *Advances in Materials and Metallurgy*. Springer Singapore, 2019.
- [18] J. Bijwe and M. Kumar, “Optimization of steel wool contents in non-asbestos organic (NAO) friction composites for best combination of thermal conductivity and tribo-performance,” *Wear*, vol. 263, no. 7–12 SPEC. ISS., pp. 1243–1248, 2007.
- [19] H. J. Hwang, S. L. Jung, K. H. Cho, Y. J. Kim, and H. Jang, “Tribological performance of brake friction materials containing carbon nanotubes,” *Wear*, vol. 268, no. 2–3, pp. 519–525, 2010.
- [20] M. Robere, “Disc Brake Pad Corrosion Adhesion: Test-to-Field Issue Correlation, and Exploration of Friction Physical Properties Influence to Adhesion Break-Away Force,” *SAE Tech. Pap.*, 2016.
- [21] M. L. Holly, L. DeVoe, and J. Webster, “Ferritic Nitrocarburized Brake Rotors,” 2011.
- [22] M. A. Sai Balaji, K. Kalaichelvan, “Optimization of a non asbestos semi metallic disc brake pad formulation with respect to friction and wear,” *Procedia Eng.*, vol. 38, pp. 1650–1657, 2012.
- [23] R. Vijay, M. Jeeshanesh, M. A. Saibalaji, and V. Thiyagarajan, “Optimization of tribological properties of Nonasbestos brake pad material by using steel wool,” *Adv. Tribol.*, vol. 2013, 2013.
- [24] P. J. Blau, “Compositions, Functions, and Testing of Friction Brake Materials and Their Additives,” *Energy*, vol. 27, no. September, p. 38, 2001.
- [25] U. S. Hong, S. L. Jung, K. H. Cho, M. H. Cho, S. J. Kim, and H. Jang, “Wear mechanism of multiphase friction materials with different phenolic resin matrices,” vol. 266, pp. 739–744, 2009.
- [26] Z. Zhu *et al.*, “Friction and Wear Behavior of Resin/Graphite Composite under Dry Sliding,” *J. Mater. Sci. Technol.*, vol. 31, no. 3, pp. 325–330, Mar. 2015.
- [27] B. Surya Rajan, M. A. Sai Balaji, and C. Velmurugan, “Correlation of field and experimental test data of wear in heavy commercial vehicle brake liners,” *Friction*, vol. 5, no. 1, pp. 56–65, 2017.
- [28] V. D. A. Čirović, “Dynamic Modelling of Disc Brake Contact Phenomena,” *FME Trans.*, vol. 39, pp. 177–183, 2011.

- [29] P. D. Neis, N. F. Ferreira, G. Fekete, L. T. Matozo, and D. Masotti, "Towards a better understanding of the structures existing on the surface of brake pads," *Tribol. Int.*, vol. 105, pp. 135–147, 2017.
- [30] M. H. Cho, K. H. Cho, S. J. Kim, D. H. Kim, and H. Jang, "The role of transfer layers on friction characteristics in the sliding interface between friction materials against gray iron brake disks," *Tribol. Lett.*, vol. 20, no. 2, pp. 101–108, 2005.
- [31] R. A. Al-Samarai, H. , K. R. Ahmad, and Y. Al-Douri, "Evaluate the Effects of Various Surface Roughness on the Tribological Characteristics under Dry and Lubricated Conditions for Al-Si Alloy," *J. Surf. Eng. Mater. Adv. Technol.*, vol. 02, no. 03, pp. 167–173, 2012.
- [32] M. Eriksson, S. Jacobson, "Tribological surfaces of organic brake pads," *Tribol. Int.*, vol. 33, no. 12, pp. 817–827, Dec. 2000.
- [33] K. W. Liew and U. Nirmal, "Frictional performance evaluation of newly designed brake pad materials," *Mater. Des.*, vol. 48, pp. 25–33, 2013.
- [34] K. Kendall, "Adhesion and composites," *Compos. Interfaces*, vol. 4, no. 5, pp. 299–311, 1996.
- [35] H. Jang, K. Ko, S. . Kim, R. . Basch, and J. . Fash, "The effect of metal fibers on the friction performance of automotive brake friction materials," *Wear*, vol. 256, no. 3–4, pp. 406–414, Feb. 2004.
- [36] V. Thiyagarajan, K. Kalaichelvan, R. Vijay, and D. Lenin Singaravelu, "Influence of thermal conductivity and thermal stability on the fade and recovery characteristics of non-asbestos semi-metallic disc brake pad," *J. Brazilian Soc. Mech. Sci. Eng.*, vol. 38, no. 4, pp. 1207–1219, Apr. 2016.
- [37] F. Wang and Y. Liu, "Mechanical and tribological properties of ceramic-matrix friction materials with steel fiber and mullite fiber," *Mater. Des.*, vol. 57, pp. 449–455, 2014.
- [38] M. D. Bryant, "Entropy and dissipative processes of friction and wear," *FME Trans.*, vol. 37, no. 2, pp. 55–60, 2009.
- [39] G. P. Ostermeyer, "Friction and wear of brake systems," *Forsch. im Ingenieurwes.*, vol. 66, no. 6, pp. 0267–0272, 2001.
- [40] M. Kchaou, A. R. Mat Lazim, A. R. Abu Bakar, J. Fajoui, R. Elleuch, and F. Jacquemin, "Effects of Steel Fibers and Surface Roughness on Squealing Behavior of Friction Materials," *Trans. Indian Inst. Met.*, vol. 69, no. 6, pp. 1277–1287, 2016.
- [41] B. Surya Rajan, Balaji, M. A. S Sathickbasha, K Hariharasakthisudan, "Influence of Binder on Thermomechanical and Tribological Performance in Brake Pad," *Tribol. Ind.*, vol. Accepted f, 2018.
- [42] L. Matějka, G. Simha Martynková, Y. Ma, and Y. Lu, "Semimetallic brake friction materials containing ZrSiO₄: Friction performance and friction layers evaluation," *J. Compos. Mater.*, vol. 43, no. 13, pp. 1421–1434, 2009.
- [43] P. Chandra Verma, L. Menapace, A. Bonfanti, R. Ciudin, S. Gialanella, and G. Straffelini, "Braking pad-disc system: Wear mechanisms and formation of wear fragments," *Wear*, vol. 322–323, pp. 251–258, 2015.

УТИЦАЈ ПОРОДИЦЕ ЧЕЛИЧНИХ ВЛАКАНА НА ТРЕЊЕ И СТАТИЧКО ТРЕЊЕ КОД КОЧИОНИХ ОБЛОГА

Сатикбаша К., Селвакумар А. С.,
Сал Балаћи М. А., Сурја Рајан Б.

Анализира се утицај породице челичних влакана на термомеханичка, триболошка и корозивна својства фриксионог материјала на бази фенолних смола. Триболошка испитивања су извршена на машини за тестирање трења у складу са САЕ J661 стандардима. Блокада кочница (статичко трење услед корозије) је испитано према стандарду ИСО 6315. Испитивање је обухватило три типа влакана: меког челика, жареног челика и нерђајућег челика. Процент тежине влакана код свих композита је био константно 12% (серије са ниским садржајем метала). У циљу поређења коришћен је још један композит са 24% тежине влакана нерђајућег челика (висок проценат садржаја метала). Експерименти су показали да, опште узев, коефицијент трења опада са повећањем температуре до 300⁰Ц и да се потом стабилизује. Композити ојачани влакнима меког челика се понашају боље у погледу карактеристика прегревања и хабања. Следе композити ојачани влакнима нерђајућег челика. Већи проценат трења (мале конзистенције) и хабања имали су композити са већим процентом влакана нерђајућег челика. Механизам хабања је испитиван скенирајућом електронском микроскопијом.